Nonlinear Distortion Mitigation with Non-Orthogonal DFT-precoding for DML-Based OFDM Optical Systems

Peiji Song[1], Zhouyi Hu[2,*], Yizhan Dai[1], and Chun-Kit Chan[1]
[1]*Department of Information Engineering, The Chinese University of Hong Kong, Shatin, N.T., Hong Kong, China*
[2]*Aston Institute of Photonic Technologies, Aston University, Birmingham, B4 7ET, United Kingdom*
[*]*E-mail: z.hu6@aston.ac.uk*

Abstract: We propose to use non-orthogonal DFT-matrix precoding to mitigate the nonlinear distortion induced by chirp and fiber dispersion in a 10-Gb/s DML-based OFDM optical system, with 0.83-dB sensitivity improvement over the third-order Volterra nonlinear equalizer. © 2022 The Author(s)

1. Introduction

Intensity modulation and direct detection (IM/DD) optical system has been extensively studied as a promising solution for optical metro networks and data center networks, due to its low cost and low complexity [1]. To further reduce the system complexity, directly modulated laser (DML) is preferred over other external modulators, such as electro-absorption modulators (EAM) and Mach-Zehnder modulators (MZM). With the merits of flexible modulation and resilience to fiber chromatic dispersion (CD) brought by orthogonal frequency division multiplexing (OFDM), the DML-based OFDM technique has recently attracted considerable attention to realize practical IM/DD optical systems [2]. However, DML suffers from strong frequency chirp, which induces severe nonlinear distortion when interacting with CD. Previous approaches of nonlinear distortion mitigation include subcarrier-to-subcarrier intermixing interference (SSII) cancellation [3] and Volterra nonlinear equalizers (VNLE) [4]; however, they have limited performance or high complexity. As the nonlinear distortion is mainly distributed at the low frequency range, a gapped-OFDM technique [2] was proposed to discard those low frequency subcarriers with low signal-to-noise ratio (SNR) and maximize the capacity by applying the adaptive bit and power loading (ABPL) algorithm to the rest of the subcarriers. Although this gapped-OFDM outperforms the conventional OFDM incorporating the third-order VNLE, it suffers from high system complexity and latency, hindering its applications to practical systems.

In this paper, we propose to employ the gapped-OFDM technique but the ABPL is replaced by the recently proposed non-orthogonal discrete Fourier transform precoding (NODFT-p) [5]. It can reduce the system complexity, lantency, and keep spectral efficiency unchanged compared with conventional OFDM signal. The pre-coded subcarriers are allocated at the high frequency range, in contrast with that in [5], to generate the required gap. With this new precoding technique, we have experimentally demonstrated a 9.5-Gb/s QAM-4 optical signal transmission over a 100-km standard single mode fiber (SSMF) for the proof-of-concept. The results show that the NODFT-p pre-coded gapped-OFDM signal achieves 4.9-dB and 0.83-dB sensitivity improvement over the conventional OFDM signal without and with the *T*/2-spaced third-order VNLE, respectively, while the respective reduction in the computation complexity is up to 91.15% (multiplications) and 86.74% (additions).

2. Principle of NODFT-p Gapped-OFDM

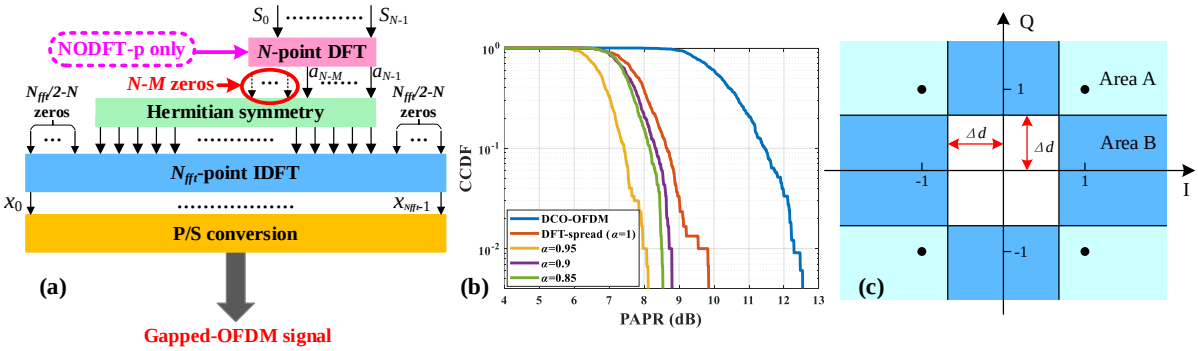

Fig. 1. (a) Principles of the gapped-OFDM, (b) mapping strategy of QAM-4 constellation, and (c) CCDF of PAPR for different signals, where 230/512 subcarriers are effectively modulated by QAM-4 symbols.

Fig. 1(a) illustrates the principles of the gapped-OFDM. For the conventional gapped-OFDM, the *M* subcarriers $\{a_{N-M}, a_{N-M+1}, \ldots, a_{N-1}\}$ carry the symbols obtained with ABPL, leaving the (*N*-*M*) subcarriers $\{a_0, a_1, \ldots, a_{N-M-1}\}$ as the gap.

However for the NODFT-p gapped-OFDM, the M subcarriers $\{a_{N-M}, a_{N-M+1}, \ldots, a_{N-1}\}$ are compressed from the N subcarriers $\{S_0, S_1, \ldots, S_{N-1}\}$ by an $M\times N$ ($M\leqslant N$) NODFT matrix, where its (m,n)-th entry is denoted by $\boldsymbol{W}_{m,n}=\exp(-j2\pi mn/N)/\sqrt{(M)}$, for m=0, 1, …, (M-1), and n=0, 1, …, (N-1), where the compression factor α is defined by $\alpha=M/N$. Note that $\boldsymbol{W}$ is equivalent to the standard DFT matrix when α=1 (M=N). The value of M must be optimized to get the best transmission performance during the experiment. Herein, we set the number of subcarriers before NODFT-p equal to that used in the conventional OFDM system to keep the spectral efficiency unchanged. An inverse NODFT (INODFT) matrix $\boldsymbol{W}^{\mathrm{H}}$ is employed for decoding at the receiver side, which is the Hermitian transpose of $\boldsymbol{W}$.

Fig. 1(b) shows the complementary cumulative distribution function (CCDF) of the peak-to-average-power-ratio (PAPR) curves for different signals, showing the much-reduced PAPR of the proposed NODFT-p gapped-OFDM signal over the conventional OFDM case.

Since the matrix $\boldsymbol{W}$ and $\boldsymbol{W}^{\mathrm{H}}$ are no longer orthogonal, the inter-carrier interference (ICI) is purposely induced. Thus, the cascaded binary-phase-shift-keying iterative detection (CBID) [5] is an effective algorithm to mitigate ICI based on the correlation matrix $\boldsymbol{C}$, where the (i, k)-th entry of $\boldsymbol{C}$ is given by,

$$\boldsymbol{C}_{i,k}=\boldsymbol{W}^{\mathrm{H}}\boldsymbol{W}=\sum_{m=0}^{M-1}\exp(-j2\pi m(k-i)/N)/M. \quad (1)$$

In the i-th iteration of CBID, the received symbols $\boldsymbol{S}_i$ after the INODFT matrix decoding is first updated by,

$$\boldsymbol{S}_i=\boldsymbol{R}+(\boldsymbol{I}-\boldsymbol{C})\boldsymbol{S}_{i-1}, \quad (2)$$

where $\boldsymbol{R}$ is the decoded symbols after the INODFT matrix, $\boldsymbol{I}$ is the identity matrix, and $\boldsymbol{S}_{i-1}$ is the symbols after (i-1)-th iterations. As depicted in Fig. 1(c), the symbols located inside area A and area B after the above iterations are mapped onto the corresponding constellation points, while leaving other symbols unchanged until the next iteration. The threshold interval during the iteration is changed as Δd=1-i/L, where L is the total number of iterations.

3. Experimental setup and results

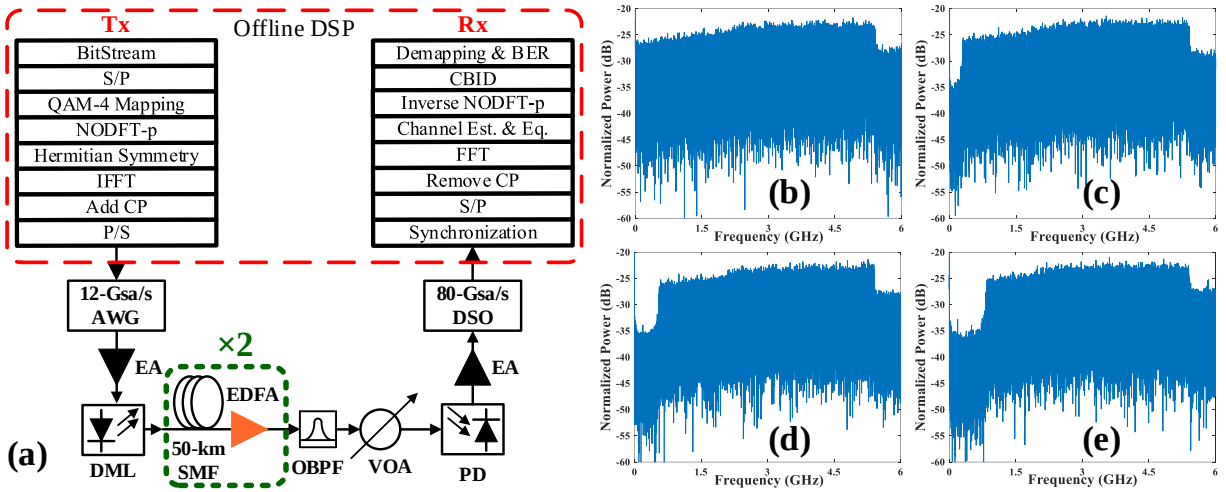

Fig. 3 (a) Experimental setup and DSP of the proposed NODFT-p gapped-OFDM. (b) – (e): Electrical spectra of the received signals with compression factors of (b) 1, (c) 0.95, (d) 0.9, and (e) 0.85, respectively.

Fig. 3(a) shows the experimental setup and the digital signal processing (DSP). At the transmitter, the bit-stream after serial-to-parallel conversion (S/P) was first mapped onto QAM-4 symbols, which were allocated over 230 subcarriers (N=230), and then transformed into M subcarriers by the NODFT matrix. Hermitian symmetry was applied before performing a 512-point inverse fast Fourier transform (IFFT) for the generation of a real-valued signal. Then, a cyclic prefix (CP) with a length of 16 was added to combat CD. To estimate the channel response and implement equalization at the receiver, 30 blocks of QAM-4 training sequences (TS) were added before the 300 blocks of OFDM payload symbols. A 12-GSa/s arbitrary waveform generator (AWG) together with a DML at a center wavelength of 1546.2 nm converted the digital signal into an optical signal, where the bias current and the driving voltage of the DML were set to 80-mA, and 500-mV, respectively. Therefore, the data rate of the signal is 9.5($\approx$12×2×230/512×512/528×300/330) Gb/s. After 100-km SSMF transmission, an optical bandpass filter (OBPF) was employed at the second erbium-doped fiber amplifier (EDFA) output to suppress the out-of-band amplified spontaneous emission noise. A variable optical attenuator (VOA) was used to measure the sensitivity curve. The signal was detected by a 40-GHz photodiode (PD) and finally captured by a real-time oscilloscope operating at 80-GSa/s for offline DSP.

Fig. 3(b)-(e) present the electrical spectra of the received NODFT-p gapped-OFDM signals with different values of α. We can notice that the gap width increases as α decreases. Fig. 4(a) shows the calculated SNR profile of our system. Compared with the back-to-back (BTB) case, the SNR of the subcarriers at the low frequency range is greatly degraded after the 100-km SSMF transmission, due to the nonlinear distortion. Therefore, abandoning these subcarriers is helpful to alleviate the impairment; however, the ICI increases as the gap width increases, which may result in the loss of the subcarriers with high SNR. Therefore, an optimal gap width exists to fully utilize the subcarriers suitable for data transmission. Fig. 4(b) depicts the optimization of the gap width, where the optimal gap width is obtained at α=0.95, corresponding to ~0.28 GHz, and the respective optimal number of iterations L is 3.

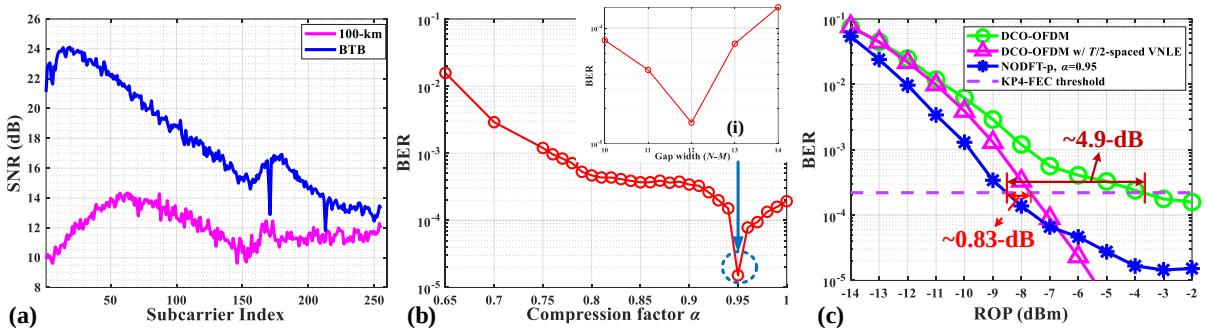

Fig. 4 (a) Calculated SNR at ROP=−2-dBm, (b) measured BER versus α at ROP=−2-dBm after 100-km SSMF transmission, and (c) measured transmission performance after a 100-km SSMF transmission. Inset (i): BER versus the value of (N-M) around α=0.95.

Fig. 4(c) shows the measured received optical power (ROP) sensitivity for the received signals, benchmarked with conventional techniques. The proposed scheme with the optimal gap width always outperforms the conventional OFDM case. Moreover, we also compared it with the conventional OFDM signal incorporating a T/2-spaced recursive least square (RLS)-based third-order VNLE. Note that only the diagonal terms of the third-order terms are included in the third-order filtering to reduce the complexity, as the distortion is mainly of the second order. The optimal tap number of this third-order VNLE was set to (83, 15, 7). As shown in Fig. 4(c), the proposed scheme achieves a 0.83-dB sensitivity improvement over the VNLE case at the KP4-FEC threshold. Besides, the computation complexity is reduced by 91.15% (multiplications) and 86.74% (additions). Fig. 5 shows the constellations of the different signals. We can see that the constellations with the proposed scheme are more precise than others.

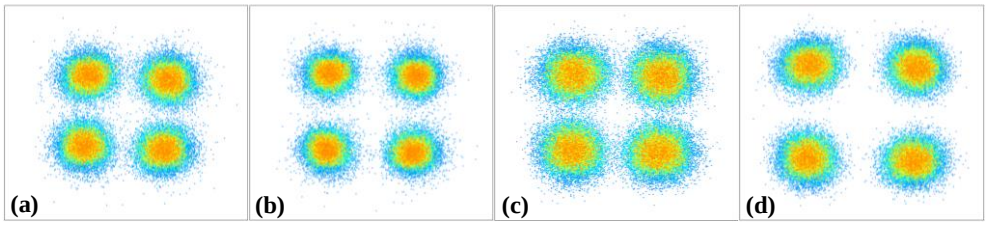

Fig. 5 Constellations of conventional OFDM signal (a) without VNLE, (b) with third-order VNLE, and NODFT-p gapped OFDM signal (c) without ICI mitigation, and (d) with ICI mitigation, at ROP=-8dBm.

4. Summary

We have proposed the NODFT-p gapped-OFDM technique to mitigate the nonlinear distortion in a DML-based OFDM transmission system. Experimental results show a 0.83-dB sensitivity improvement and up to 91.15% (multiplications) and 86.74% (additions) reduction in computation complexity, compared with T/2-spaced RLS-based third-order VNLE.

5. References

[1] Q. Cheng et al., "Recent advances in optical technologies for data centers: a review," *Optica* vol. 5, pp. 1354-1370 (2018).
[2] H. M. Nguyen et al., "Reducing the impact of nonlinear distortion in DML-Based OFDM transmission by frequency gap," *J. Lightwave Technol.*, Vol. 36, pp. 5617-5625 (2018).
[3] D. Z. Hsu et al., "Cost-effective 33-Gbps intensity modulation direct detection multi-band OFDM LR-PON system employing a 10-GHz-based transceiver," *Optics Express*, Vol. 19, pp. 17546-17556 (2011).
[4] N. S. André et al., "Adaptive nonlinear Volterra equalizer for mitigation of chirp-induced distortions in cost effective IMDD OFDM systems," *Optics Express*, Vol. 21, pp. 26527-26532 (2013).
[5] Z. Hu, and C. K. Chan, "Non-orthogonal matrix precoding based faster-than-Nyquist signaling over optical wireless communications," in *Optical Fiber Communication Conference (OFC)* 2020, OSA Technical Digest (Optical Society of America, 2019), paper W1J.5.